Available online at www.sciencedirect.com
SCIENCE DIRECT
Chemical Physics Letters 418 (2006) 152–157
CHEMICAL PHYSICS LETTERS
www.elsevier.com/locate/cplett

Structural evolution of AlN nano-structures: Nanotips and nanorods

Shih-Chen Shi [a], Surojit Chattopadhyay [b,*], Chia-Fu Chen [a], Kuei-Hsien Chen [b,c], Li-Chyong Chen [c]

[a] Department of Materials Science and Engineering, National Chiao Tung University, Hsinchu 300, Taiwan
[b] Institute of Atomic and Molecular Sciences, Academia Sinica, 1, Roosevelt Road, Section 4, P.O. Box 23-166, Taipei 106, Taiwan
[c] Center for Condensed Matter Sciences, National Taiwan University, Taipei 106, Taiwan

Received 10 June 2005; in final form 8 September 2005
Available online 16 November 2005

Abstract

Aluminum nitride (AlN) nanostructures were prepared using thermal chemical vapour deposition process. At growth temperatures of 950 °C, AlN nanotips with apex diameters of 10 nm, base diameters of ~100 nm, and length of ~2000 nm were obtained. Whereas when the growth temperature was 1200 °C, we obtained shorter and thicker AlN nanorods. Compelling microscopic evidences were obtained to show that stacked AlN platelets of diminishing size formed the building blocks for the nanotips. A reducing Ehrlich–Schwoebel barrier introduced into a diffusion mediated growth model explains the formation of AlN nanorods at increasing growth temperatures.

1. Introduction

Synthesis of nanoscaled materials with defined electrical and mechanical properties will enable the realization of practical applications. But of fundamental importance is the knowledge of their growth mechanism. For example, the vapour–liquid–solid (VLS) growth mechanism proposed by Wagner and Ellis [1] to explain whisker growth has remained a landmark. Group III-nitrides is arguably the most sought-after class of materials owing to the range of properties they encompass. Aluminium nitride (AlN) is a hard ceramic material with a wide band gap and can be subjected to high stress, high temperature, and a corrosive environment. Various chemical and physical deposition techniques have reportedly created oriented structures of AlN nanotubes, nanobelts and nanowires with average diameters typically ranging from 20 to 100 nm, and lengths up to 100 μm [2–4]. AlN nanotips (AlNNTs) were also reported recently by two groups [5,6]. Conical nanotubules of graphite [7], boron nitride [8] and indium nitride [9] systems has been reported and few reports also attempted to give a growth model for the conical morphologies [6,10–12]. However, the formation of a solid tip structure, unlike the conical tubule, is intriguing and a comprehensive growth model is lacking. The growth model proposed in [6] is inadequate from the atomistic point of view as will be discussed later also. In one report for the vapour–liquid–solid (VLS) growth of GaAs [13], a conical structure was really observed at low growth temperatures (T_d) but was attributed to a non-uniform diffusion mediated growth along the side walls. Here we report on the synthesis of crystalline AlN nano-structures by the thermal chemical vapour deposition (CVD) route. This work investigates the effect of T_d on the shape evolution of the resultant AlN nano-structures. We propose a growth model that takes into account an effective diffusion length of adatoms, the Ehrlich–Schwoebel barrier [14,15] for adatoms hopping down a step, and strain induced in the growing lattice for the shape evolution.

2. Experimental

AlN nano-structures were fabricated by vaporizing Al powders under ammonia (NH_3) environment in a tubular furnace by atmospheric pressure thermal CVD technique

* Corresponding author. Fax: +886 2 23655404.
E-mail address: sur@diamond.iams.sinica.edu.tw (S. Chattopadhyay).

0009-2614/$ - see front matter © 2005 Elsevier B.V. All rights reserved.
doi:10.1016/j.cplett.2005.10.107

[16,17]. The growth proceeds via vapor transport and condensation process (VTCP) [5,18]. The reaction chamber was heated up to 950–1200 °C and kept there for a period of 30 min during the process. Nanostructures, produced on the silicon substrates at different temperatures set-points controlled between 950 and 1200 °C, were studied. The morphology, structure and composition of the samples were studied using scanning electron microscopy (SEM, JEOL 6700 FESEM), transmission electron microscopy (TEM, JEOL JEM 40000 EX), Raman spectroscopy (Renishaw 2000, UK), and X-ray diffraction (XRD) analysis.

3. Results and discussion

A series of experiments were carried out to study the effect of T_d variation on the shape evolution of the AlN products. Fig. 1a–d shows SEM images of AlN nanoproducts grown for 30 min on the Au coated Si substrates at different T_d of 950, 1000, 1100, and 1200 °C, respectively. At $T_d = 950$ °C, the AlN nanotips evolved (Fig. 1a). As T_d increased, a (0 0 1) facet (c-facet) appeared on the top of the nanotips, forming a flat section at the top instead of the tip shape. The area of this (0 0 1) facet increased with increasing T_d as shown in Fig. 1b–d. As shown clearly in Fig. 1d, $T_d = 1200$ °C produced AlN nanorod which has a simple six-sided faceted structure. The cross-section of the nanotips and nanorods were both hexagonal.

The cross-sectional SEM images of the nanotips and nanorods shown in Fig. 2a,b, respectively, indicates their relative dimensions. The inset of Fig. 2a,b depict the early stages of growth of the nanotips and nanorods, respectively. It indicates that the shapes of the AlN nano-structures were probably decided at the very early stages of the growth. Fig. 2c represents the X-ray diffraction analysis of the AlN nanostructures. It shows the strongest reflection of the (0 0 2) plane compared to (1 0 0) and (1 0 1) of the h-AlN (JCPDS 25–1133), indicating a preferential growth perpendicular to the basal plane along [0 0 1]. The Raman spectra of the nanotips and nanorods, as shown in Fig. 2d, were collected using Ar^+ laser as the excitation source. Three clear Raman-active phonon modes can be observed. These are in agreement with those of the h-AlN crystal [19].

The shape evolution of the AlN nanostructures as a function of T_d is interesting as the result (Fig. 1) shows. The digestion of the results presented in this letter as well as our earlier work on nanotips [5,20] yields certain observations as listed below:

Observation 1: No metallic gold was found at the apex of the AlN nanotip, and some remnant non-nitrided Al was present at the very base of the structure [5].

Observation 2: The body of the nanostructure is purely hexagonal AlN growing along [0 0 1] and no metallic Al phase is present [5,20].

Observation 3: A high aspect ratio (>10) nanotip structure, having apex angles of ~18°, produced at $T_d = 950$ °C modifies into a low aspect ratio (~5) flat top ((0 0 1) facet) nanorods at $T_d = 1200$ °C.

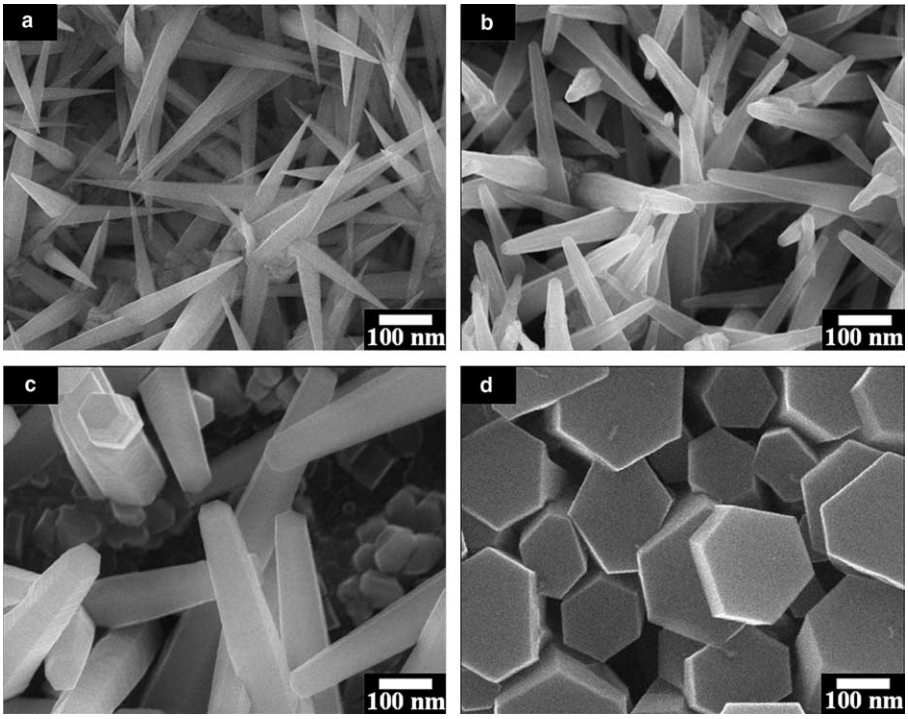

Fig. 1. Typical SEM images of the AlN nanostructures on silicon substrates (coated with 15 nm of gold) grown under (a) 950 °C, (b) 1000 °C, (c) 1100 °C, and (d) 1200 °C, respectively.

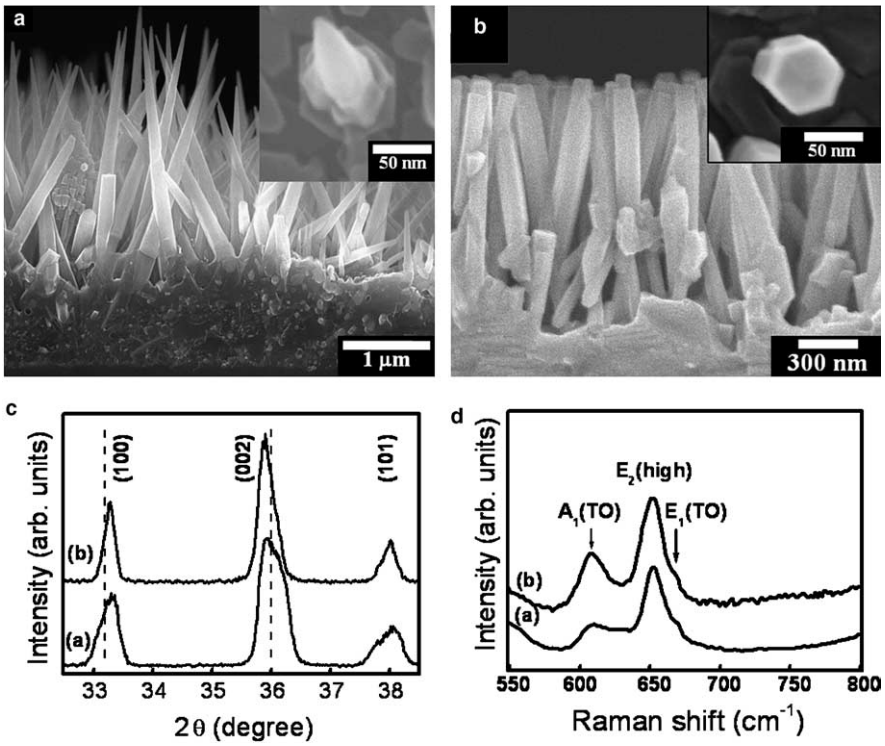

Fig. 2. Typical cross-section SEM image of AlN nanostructures grown on 15 nm Au coated Si substrate under (a) 950 and (b) 1200 °C, respectively. Inset (a) and (b) show the SEM image of AlN nano-product grown for 25 min, respectively. (c) Typical XRD and (d) Raman spectra taken from the AlN nanostructures in figure (a) and (b), respectively. The two vertical dashed lines in figure (c) represent bulk AlN positions for (100) and (002) reflections (JCPDS Card No. 25–1133).

Any proposed growth model should explain these listed observations of which the last one is of most importance.

We begin with a discussion on a diffusion mediated growth mechanism which is the most obvious as we are dealing with a temperature activated process. The growth of AlN nanostructures proceeds by the transport of Al vapours to the growth region as the temperature inside the quartz tube is ramped up. Note, although a thin Au layer was used on the Si substrate, it was not detected at the tip of the nanostructures or in its body. Again the nanotips could be obtained even without any Au catalyst on the substrate [5]. This allowed us to exclude a VLS mechanism and pursue the vapour–solid (VS) route instead. We introduce a diffusion mediated growth mechanism here. Al vapours landing on the growth surface will migrate with a large diffusion length, L_{Al}, and can be adsorbed as Al droplets or wetting layer on the gold particles when T_d is low (but above 660 °C, the melting point of Al powders). As the T_d of 950 °C is reached, NH_3 dissociates and the N-flux increases on the Al droplet nitriding it. When $T_d = 950$ °C, the Al vapours will react with NH_3 or its dissociation products producing AlN following Eq. (1) initiating the VS process:

$$2Al + 2NH_3 = 2AlN + 3H_2,$$
$$\Delta G = -9.7 \text{ kJ/mol at } 950^\circ C,$$
$$\Delta G = -14.6 \text{ kJ/mol at } 1200^\circ C. \quad (1)$$

Then AlN will migrate with a diffusion length, L_{AlN}. Consequently, an effective diffusion length L_{eff} is defined as

$$L_{eff} = L_{Al} + L_{AlN}, \quad (2)$$

where L_{Al} and L_{AlN} are temperature activated according to the following [21]:

$$L_{Al} \sim t_{Al}^{1/2} \exp\left(-\frac{E_{Al}}{2k_B T}\right), \quad (3)$$

$$L_{AlN} \sim t_{AlN}^{1/2} \exp\left(-\frac{E_{AlN}}{2k_B T}\right), \quad (4)$$

where t and E are the diffusion times and activation energies for surface diffusion, respectively, and k_B is the Boltzmann constant. The AlN can be deposited at a low energy site and contribute to the growth. This happens in a condition close to $t_{Al} \sim t_{AlN}$, and $L_{Al} \sim L_{AlN}$. The nitridation of the Al may be partial leaving some remnant metallic Al in this seed. Also at the high T_d, evaporation and subsequent removal of both metallic Au and Al is possible. The Au is thus not taking part in either a tip- or root-mediated VLS process and is not observed in the nanotip body explaining observation 1. Above the dissociation temperature of NH_3 the thermodynamics of the system (negative Gibb's free energy for Eq. (1)) promotes the formation of AlN crystallizing in the wurtzite structure. This explains observation 2.

To address observation 3 we discuss the anisotropy as well as strains that might be present during the growth.

The initial AlN islands may have edges beveled at an angle θ, with respect to the substrate, determined by the surface energetics [22]. Let us discuss first the diameters of the AlN nanostructures grown at different T_d. From our TEM and XRD results we have already established that we have a [0 0 1] growth direction for all kinds of nanostructures grown at different T_d. Number of dangling bonds available per oncoming growth precursors on the Al(0 0 1) and N(0 0 $\bar{1}$) faces are 3 and 1, respectively (Fig. 3a). The lateral facets have two kinds of surfaces, namely A and B, which have 2 and 1 dangling bonds, respectively, per oncoming growth species (Fig. 3b). Hence on the average each growth precursor has 1.5 dangling bonds available for bonding on the lateral faces. Evidently, based on the availability of dangling bonds, diffusion lengths on the lateral faces of the hexagonal islands will be less than that on the N-terminated (0 0 $\bar{1}$) face [23]. This will lead to an anisotropy in the growth rates resulting in large platelets/islands of AlN following Eq. (1). Since the diffusion length is temperature activated, a larger T_d will produce larger but thin platelets. This exactly explains why the nanotips produced at 950 °C (Fig. 1a) had smaller base diameters than the nanorods (Fig. 1d) prepared at 1200 °C. However, this also means that the nanorods are closer to equilibrium than the nanotips which is understandable because of a larger diffusion length of the AlN precursors at higher T_d. Following the model proposed by Tersoff and Tromp [22], the island size (a_0) is related to the surface energy (Γ) and a stress factor (c) by the following:

$$a_0 = e\xi h e^{\frac{\Gamma}{ch}}, \tag{5}$$

where h is the height of the initial island and $\xi = e^{-1.5}\cot\theta$. This model predicts that if $ch \gg \Gamma$, then the island sizes a_0 will be smaller. So the nanotips having a smaller base diameter are the stressed ones. However, the model presumed a slant edge ($\theta \neq 90°$) island and cannot directly predict a perfect ($\theta = 90°$) wide base rod-like crystal, since then $\xi = 0$ and $a_0 \to 0$. There are indications that such perfect ($\theta = 90°$) islands [24] can be the seeds for nanorod growth via the VS mechanism.

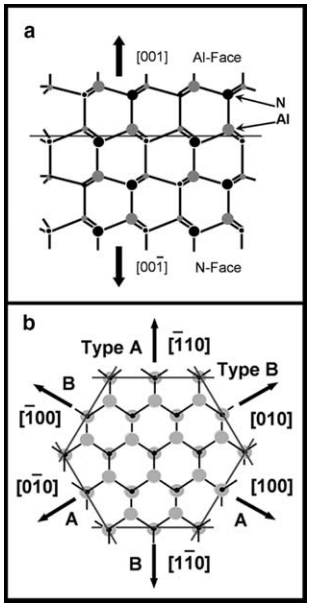

Fig. 3. (a) The cross-sectional view of hexagonal close packed wurtzite crystal structure of AlN. (b) The plan-view of a bi-layer of hcp AlN. There are two types of lateral growth directions marked as A and B.

Now consider the vertical growth of the AlN nanostructures along the [0 0 1] direction which is an Al-terminated face (Fig. 3a). For $T_d \geqslant 950$ °C, the dissociation rate of NH_3 was very fast and the Al vapor pressure was high, suggesting $t_{Al} \to 0$ and $0 \leftarrow L_{Al} \ll L_{AlN}$; so $L_{eff} = L_{AlN}$. Each incident N atom at the growth face has three available bonds connecting with three Al atoms. This means, $E_{AlN}(001) \gg E_{AlN}(00\bar{1})$ and also $E_{AlN}(001) > E_{AlN}(010)$, resulting in growth rates $R[001] > R[010] > R[00\bar{1}]$. A higher growth rate along the Al-terminated [0 0 1] direction is observed than that along the normal to the lateral faces. When this condition is satisfied, we expect an aspect ratio >1.

The beauty of crystal growth is depicted in Fig. 4. The nanotips produced at 950 °C (Fig. 4a) clearly shows a stacking of differently sized platelets along the growth direction generating the tip shape. The platelets/islands behave similar to a building block and a repetitive stacking of these, layer by layer, gives rise to the nanostructures. A similar stacking of double bi-layer steps has been observed along the sidewalls of InN pyramids also [24]. However the existence of these distinct platelets started to disappear from $T_d = 1000$ °C (Fig. 4b) signifying deposition along the lateral facets of the platelets. A significant portion of this deposition may be due to adatom hopping down a step. Fig. 4a–d demonstrates the growth along the radial direction of the nanostructures due to adatom hopping as a result of a reducing Ehrlich–Schwoebel barrier, and increased diffusion length as T_d is increased. When $T_d = 1100$ °C, the top (0 0 1) facet clearly appears and the lateral growth becomes more pronounced giving it a smoother appearance than that observed during 1000 °C. However the conical nature of the structure is still maintained. As T_d creeps up to 1200 °C, the diffusion length was sufficient to push the system towards equilibrium resulting in larger hexagonal platelets and growth along the lateral facets generating the pillar like structure of the nanorods with a near perfect uniformity in diameter. Note that the existence of the Ehrlich–Schwoebel barrier at low T_d will also give rise to a large driving force along the [0 0 1] growth direction [25,26]. In addition, the stress along the basal plane of the platelets, as indicated from the smaller base diameters of the nanotips, is also known to drive the growth along a direction perpendicular to it. This explains why the nanotips have a higher aspect ratio than the nanorods.

Lastly, the origin of the tip shape has to be addressed for the growth at 950 °C. Since the growth units were clearly identified as islands/platelets stacked on each other, it is only obvious that a certain arrangement of these produced

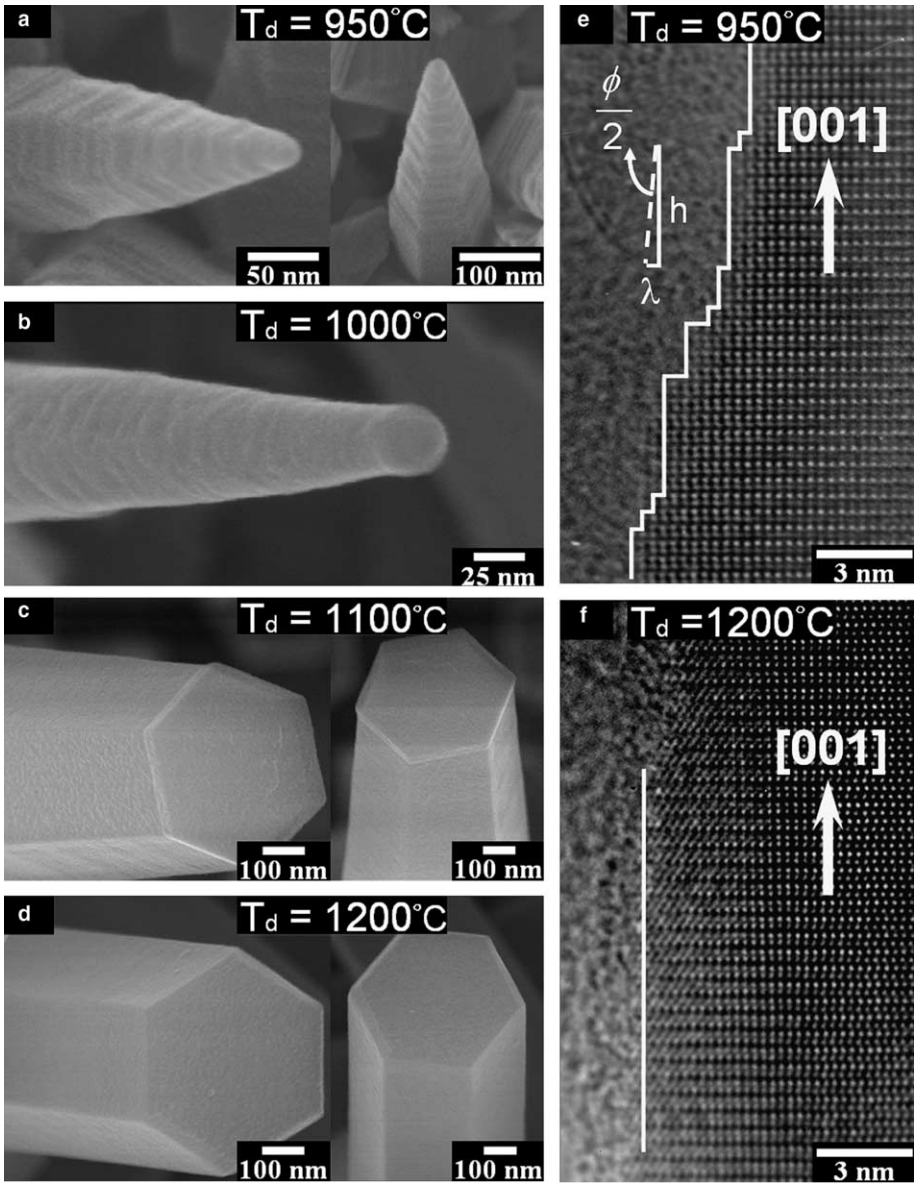

Fig. 4. (a–d) High resolution SEM images of the AlN nanostructures produced at different growth temperatures; (e) HRTEM image of the edge of the nanotips showing the step edges, including the step height (h) and step spacing (λ); a schematic aiding in the estimation of the semi apex angle ($\phi/2$) is also shown; (f) HRTEM image of the edge of the nanorods showing uniform diameter without tapering via step edges.

the tip shape. Careful TEM observations proved what we conjectured in our earlier work [5]. This is a pyramidal growth of 3D islands growing on top of each other (Fig. 4e). The tilted surface of the nanotips consist of a train of parallel steps of polyatomic step heights (h), with a small step spacing (λ) (Fig. 4e) and a high step density ($p = h/\lambda$) [27]. A high value of p will imply a smaller apex angle (ϕ). Clearly, $h = n_1 \times d_{0\,0\,1}$, and $\lambda = n_2 \times d_{1\,\bar{1}\,0}$, where $d_{0\,0\,1}$ and $d_{1\,\bar{1}\,0}$ are the lattice spacings along and perpendicular to the growth direction, respectively, as determined from TEM studies [5] and n_1 and n_2 are integers. The apex angle of the nanotips, as determined microscopically, is dictated by the large h/λ ratio and hence small magnitudes of the ratio, though present, are neglected. Calculating h/λ from the TEM micrograph shown in Fig. 4e we can roughly estimate a set of ϕ values for our nanotips which falls within 8–22° in agreement with that measured from the SEM/TEM images. For a particular material system the lattice spacings are constant and hence h/λ is a function of only n_1/n_2. Hence following this model, a set of apex angles for solid nanotips or pyramids of any material system (for example, GaN, InN, AlN) can be predicted based only on the n_1/n_2 ratio. The nanorods does not exhibit these step structures (Fig. 4f). The nanotip growth model proposed in [6] is inadequate in a sense that reducing precursor concentration is a general reaction feature and if the model is true should always necessarily produce nanotips, which is not the case. Our results indicate rather a stress related phenomenon for the step spacing (λ) and a high Ehrlich–Schwoebel barrier to preserve the steps that

build up the nanotips. The positions for the (0 0 2) (axial) and (1 0 0) (equivalent to $[1\bar{1}0]$) reflections from the nanostructures are shifted towards lower and higher 2θ values, respectively, from their bulk counterparts as marked in Fig. 2c demonstrating tensile and compressive stress, respectively. The nanorods produced at 1200 °C manages to counter the stress deformation while nanotips produced at a lower temperature yields to it by getting tapered as growth progresses.

4. Conclusion

To summarize, the growth of high purity and dense hexagonal AlN nanotips and nanorods via a thermal chemical vapor deposition system has been demonstrated. A single growth parameter, namely the growth temperature, is able to dictate the formation of nanotips or nanorods in this vapour transport and condensation process. The AlN nanotips and nanorods grow by vapor solid mechanism and their preferred growth direction (long axis) is [0 0 1]. A diffusion mediated growth model incorporating stacking of hexagonal platelets as growth units and an Ehrlich–Schwoebel barrier at the step edge has been proposed to explain the formation of high aspect ratio nanotips with substantial microscopic and structural evidence.

References

[1] R.S. Wagner, W.C. Ellis, Appl. Phys. Lett. 4 (1964) 89.
[2] Q. Wu, Z. Hu, X.Z. Wang, Y.N. Lu, X. Chen, H. Xu, Y. Chen, J. Am. Chem. Soc. 125 (2003) 10176.
[3] Q. Wu, Z. Hu, X.Z. Wang, Y. Chen, Y.N. Lu, J. Phys. Chem. B 107 (2003) 9726.
[4] Q. Wu, Z. Hu, X.Z. Wang, Y.N. Lu, K.F. Huo, S.Z. Deng, N.S. Xu, B. Shen, R. Zhang, Y. Chen, J. Mater. Chem. Soc. 13 (2003) 2024.
[5] S.C. Shi, C.F. Chen, S. Chattopadhyay, Z.H. Lan, K.H. Chen, L.C. Chen, Adv. Func. Mater. 15 (2005) 781.
[6] C. Liu, Z. Hu, Q. Wu, X. Wang, Y. Chen, H. Sang, J. Zhu, S. Deng, N. Xu, J. Am. Chem. Soc. 127 (2005) 1318.
[7] Y. Gogotsi, S. Dimovski, J.A. Libera, Carbon 40 (2002) 2263.
[8] L. Bourgeois, Y. Bando, W.Q. Han, T. Sato, Phys. Rev. B 61 (2000) 7686.
[9] L.W. Yin, Y. Bando, D. Goldberg, M.S. Li, Adv. Mater. 16 (2004) 1833.
[10] G.G. Tibbetts, J. Cryst. Growth 66 (1984) 632.
[11] D.H. Robertson, D.W. Brenner, J.W. Mintmire, Phys. Rev. B 45 (1992) 12592.
[12] F.F. Xu, Y. Bando, R. Ma, D. Goldberg, D.Y. Li, M. Miltome, J. Am. Chem. Soc. 125 (2003) 8032.
[13] A.I. Persson, B.J. Ohlsson, S. Jeppesen, L. Samuelson, J. Cryst. Growth 272 (2004) 167.
[14] G. Ehrlich, F.G. Hudda, J. Chem. Phys. 44 (1966) 1039.
[15] R.L. Schwoebel, E.J. Shipsey, J. Appl. Phys. 37 (1966) 3682.
[16] C.H. Liang, L.C. Chen, J.S. Hwang, K.H. Chen, Y.T. Hung, Y.F. Chen, Appl. Phys. Lett. 81 (2002) 22.
[17] S. Dhara, A. Datta, C.T. Wu, Z.H. Lan, K.H. Chen, Y.L. Wang, Y.F. Chen, C.W. Hsu, L.C. Chen, H.M. Lin, C.C. Chen, Appl. Phys. Lett. 84 (2004) 3468.
[18] S.C. Shi, C.F. Chen, S. Chattopadhyay, K.H. Chen, L.C. Chen, Appl. Phys. Lett. 87 (2005) 073109.
[19] M. Kuball, J.M. Hayes, A.D. Prins, N.W.A. van Uden, D.J. Dunstan, Y. Shi, J.H. Edgar, Appl. Phys. Lett. 78 (2001) 724.
[20] S. Chattopadhyay, S.C. Shi, Z.H. Lan, C.F. Chen, K.H. Chen, L.C. Chen, J. Am. Chem. Soc. 127 (2005) 2820.
[21] D.L. Smith, Thin-Film Deposition: Principles and Practice, McGraw-Hill, New York, 1995.
[22] J. Tersoff, R.M. Tromp, Phys. Rev. Lett. 70 (1993) 2782.
[23] A.M.S. ElAhi, M. He, P.Z. Zhou, G.L. Harris, L. Salamanca-Riba, F. Flet, H.C. Shaw, A. Sharma, M. Jah, D. Lakins, S.N. Mohammad, J. Appl. Phys. 94 (2003) 7749.
[24] Y.G. Cao, M.H. Xie, Y. Liu, Y.F. Ng, H.S. Wu, Appl. Phys. Lett. 83 (2003) 5157.
[25] M.F. Gyure, J.J. Zinck, C. Ratsch, D.D. Vvedensky, Phys. Rev. Lett. 81 (1998) 4931.
[26] M.D. Johnson, C. Orme, A.W. Hunt, D. Graff, J. Sudijono, L.M. Sander, B.G. Orr, Phys. Rev. Lett 72 (1994) 116.
[27] I.V. Markov, Crystal Growth for Beginners, World Scientific, Singapore, 1995.